Available online at www.sciencedirect.com
ScienceDirect
Journal of Organometallic Chemistry 693 (2008) 297–306
Journal of Organometallic Chemistry
www.elsevier.com/locate/jorganchem

# Preparation, structural characterisation and electrochemical properties of iron(0) and tungsten(0) carbonyl complexes with 1-(diphenylphosphanyl)-1′-vinylferrocene and 1-(diphenylphosphanyl)-1′-(dimethylvinylsilyl)ferrocene as P-monodentate ligands

Petr Štěpnička *

*Charles University in Prague, Faculty of Science, Department of Inorganic Chemistry, Hlavova 2030, 12840 Prague, Czech Republic*

Received 13 September 2007; received in revised form 26 October 2007; accepted 31 October 2007
Available online 7 November 2007

**Abstract**

A new organometallic phosphanylalkene, 1-(diphenylphosphanyl)-1′-(dimethylvinylsilyl)ferrocene (**2**) was prepared and—together with 1-(diphenylphosphanyl)-1′-vinylferrocene (**1**)—studied as a ligand in iron- and tungsten-carbonyl complexes. The following complexes featuring the mentioned phosphanylalkenes as P-monodentate donors were isolated and characterised by spectral methods: $[Fe(CO)_4(L\text{-}\kappa P)]$ (**4**, L = **1**; **5**, L = **2**) and *trans*-$[W(CO)_4(L\text{-}\kappa P)_2]$ (**6**, L = **1**; **7**, L = **2**). In addition, the solid-state structures of **4** and **6** have been determined by single-crystal X-ray diffraction and the electrochemical properties of compounds **1**, **2**, **4** and **6** were studied by cyclic voltammetry at platinum electrode.


*Keywords:* Ferrocene; Alkenylphosphanes; Iron; Tungsten; Electrochemistry; Structure elucidation

## 1. Introduction

Phosphane donors are the most widely used ligands in coordination chemistry and homogeneous catalysis [1]. The number of the known phosphane donors is enormous and was markedly increased via introduced functional groups that, in turn, offer a powerful tool for tuning electronic and steric properties of the resulting functionalised phosphanes [2]. In addition to phosphanes modified with polar donor groups (e.g., $NR_2$, OR, CHO, $CO_2H$, SR, heterocycles, $PO_3R_2$ and many other), a limited number of compounds bearing potentially π-donating moieties has been also reported. Phosphane **A** [3] and **B** [4] (Scheme 1) that can be regarded as simple, alkenyl-modified triphenylphosphane derivatives, represent archetypal examples of such donors. Recently the interest in phosphanylalkenes renewed, being stimulated by successful applications of the chiral representatives in enantioselective catalysis (e.g., **C** [5] and **D** [6] in Scheme 1).

In previous work, we have focused on ferrocene-based phosphanylalkenes that have not been studied in detail before [7]. So far, we have studied the coordination properties of compound **1** [8] and also described the preparation and use in catalysis of its planar chiral, 1,2-disubstituted counterparts [9]. This contribution deals with the synthesis of a $SiMe_2$-spaced analogue of **1**, viz. compound **2** [10], and the preparation, structural characterisation and electrochemistry of iron- and tungsten-carbonyl complexes involving compounds **1** and **2** as P-monodentate ligands.

## 2. Results and discussion

### 2.1. Preparation of the ligands

1-(Diphenylphosphanyl)-1′-vinylferrocene (**1**) was prepared by Wittig olefination of 1′-(diphenylphosphanyl)

* Fax: +420 221 951 253.
*E-mail address:* stepnic@natur.cuni.cz

0022-328X/$ - see front matter © 2007 Elsevier B.V. All rights reserved.
doi:10.1016/j.jorganchem.2007.10.056

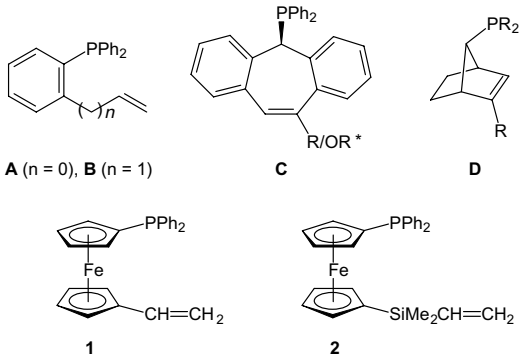


Scheme 1.

ferrocenecarboxaldehyde as previously described [8]. Its silyl-spaced analogue, 1-(diphenylphosphanyl)-1′-(dimethylvinylsilyl)ferrocene (**2**), has been obtained by sequential lithiation/functionalisation of 1,1′-dibromoferrocene [11]: the dibromide was first converted to bromide silane **3** and then phosphanylated to yield the desired phosphane silane **2** (Scheme 2). Compound **2** resulted as a viscous, amber brown oil, containing traces of side products co-eluting during chromatography (see Section 4). Exhaustive purification of **2** proved to be practically impossible due to very similar retention characteristics of the impurities. Even so, reversing the order of the reaction steps so that phosphanylation preceded the silylation led to the same product but with a considerably higher amount of the side products.

### 2.2. Complexation studies

Iron-carbonyl complexes involving ligands **1** and **2** as P-monodentate donors (**4** and **5** in Scheme 3) have been prepared by reacting equimolar amounts of the appropriate phosphane and $[Fe_2(CO)_9]$ in refluxing toluene. After solvent removal, the crude products were purified by column chromatography. Compound **4** was further crystallised from warm heptane and isolated as an air-stable, orange microcrystalline solid. On the other hand, the presence of the $SiMe_2$ spacer makes **5** and its complexes much better

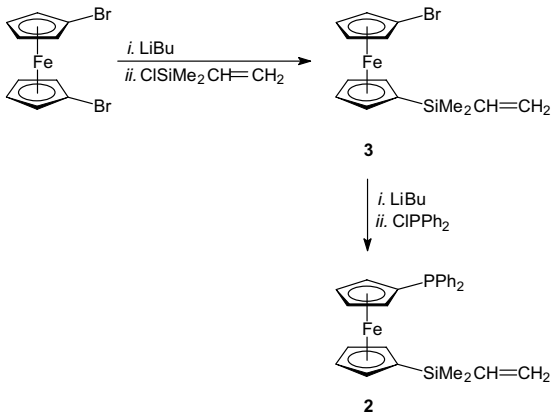


Scheme 2. Preparation of the phosphane–silane **2**.

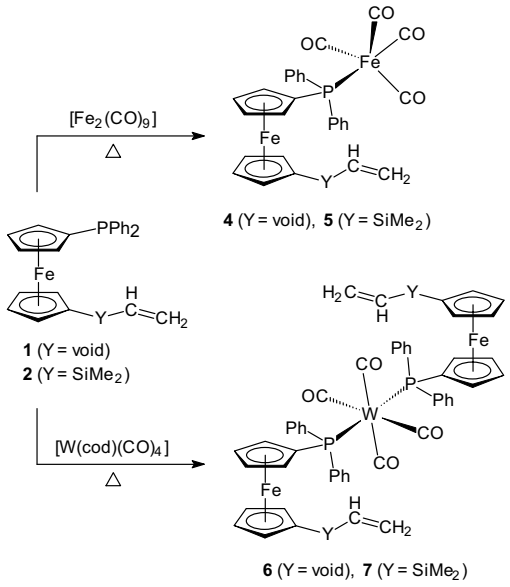


Scheme 3. Preparation of iron and tungsten complexes with ligands **1** and **2**.

soluble in common laboratory solvents, including hydrocarbons, and thus prevents purification by crystallisation. Consequently, complex **5** was isolated only by chromatography and obtained as an orange glassy solid, showing a strong tendency to retain traces of solvents.

Complexes **4** and **5** display characteristic carbonyl stretching bands in IR spectra, the pattern being similar to that of $[Fe(CO)_4(FcPPh_2\text{-}\kappa P)]$ (Fc = ferrocenyl) [12]. Their $^1H$ and $^{13}C\{^1H\}$ NMR spectra fully support the proposed formulation. The signals of the vinyl group shift only slightly upon complexation, which clearly excludes involvement of the vinyl moiety in coordination. For both compounds, the carbonyl ligands give rise to a single phosphorus-coupled doublet at $\delta_C$ ca. 213.3 with $^2J_{PC}$ = 19–20 Hz. The $^{31}P\{^1H\}$ NMR resonances of the iron complexes are shifted markedly downfield to $\delta_P$ ca. 67, which is similar to $[Fe(CO)_4(dppf\text{-}\kappa P)]$ (dppf = 1,1′-bis(diphenylphosphanyl)ferrocene; $\delta_P$ 68.4 [13] and 66.8 [14] for Fe-*P*) and, particularly, to the mono-phosphane complex $[Fe(CO)_4(Ph_2PfcCONEt_2\text{-}\kappa P)]$ ($\delta_P$ 66.9; fc = ferrocene-1,1′-diyl) [15].

The tungsten-carbonyl complexes *trans*-$[W(CO)_4(L\text{-}\kappa P)_2]$ (L = **1**, **6**; L = **2**, **7**; Scheme 3) were synthesised by refluxing the stoichiometric amounts of $[W(CO)_4(cod)]$ (cod = $\eta^2$:$\eta^2$-cycloocta-1,5-diene) and the ligand in toluene. Similarly to their iron-carbonyl counterparts, complex **6** was isolated in a 75% yield by filtration of the reaction mixture through a pad of silica gel, evaporation and subsequent crystallisation from hot heptane whilst its $SiMe_2$-homologue **7** was isolated only by column chromatography as a non-crystallising glassy solid owing to its high solubility. The latter complex is typically contaminated by $[W(CO)_5(\mathbf{2}\text{-}\kappa P)]$ (**9**, around 10%), which co-elutes during chromatography.

Attempts to prepare a 1:1 (possibly chelating) complex from [W(CO)$_4$(cod)] and **1** failed. The reaction at 1:1 mole ratio under conditions similar to the preparation of **6** afforded only a mixture of the bis(phosphane) complex **6** and unreacted **1**, whereas, at room temperature, the educts did not react at all (after 22 h in benzene-$d_6$). Likewise, a reaction between [W(CO)$_5$(MeCN)] [16] and **1** (1:1 mole ratio, in toluene at room temperature for 24 h) furnished a mixture of **6** and another product tentatively formulated as [W(CO)$_5$(**1**-κ*P*)] (**8**) on the basis of the NMR data ($\delta_P$ 11.3, s with $^{183}$W satellites, $^1J_{WP} = 246$ Hz; cf. the data for **9** and for [W(CO)$_5$(Hdpf-κ*P*)]: $\delta_P$ 10.9, $^1J_{WP} = 247$ Hz; Hdpf = 1′-(diphenylphosphanyl)ferrocenecarboxylic acid [17]).

In their $^{31}$P{$^1$H} NMR spectra, complexes **6** and **7** show singlets that are shifted downfield as compared with the free ligands ($\delta_P$ 16.3 and 16.5, respectively) and flanked with $^{183}$W satellites ($^1J_{WP} = 282$ Hz). The presence of the carbonyl ligands is manifested by a C-13 resonance at around $\delta_C$ 204, which is split into a triplet due to the interaction with two equivalent phosphorus nuclei ($^2J_{PC} = 6$ Hz). On the other hand, the carbons within to phosphorus-substituted cyclopentadienyl and phenyl rings give rise to characteristic non-binomial triplets in the $^{13}$C{$^1$H} NMR spectra as typical for virtually coupled ABX spin systems $^{12}$C–$^{31}$P(*A*)–W–$^{31}$P(*B*)–$^{13}$C(*X*) with relatively large $J_{AB}$ (or $^2J_{PP}$) values [18]. Similar features have been observed in the spectra of square-planar palladium(II) complexes involving 1′-functionalised ferrocene phosphanes as P-monodentate donors: *trans*-[PdCl$_2$(Ph$_2$PfcX-κ*P*)$_2$], where X = CO$_2$H (Hdpf) [19], PO$_3$Et$_2$ [20], and CH=CH$_2$ [8]. The NMR spectra clearly confirm the presence of uncoordinated double bonds (cf. the data for **6**; $^1$H NMR: three double doublets at $\delta_H$ 4.93, 5.18, and 6.12 of an AMX spin system with characteristic coupling constants; $^{13}$C NMR: two signals at $\delta_C$ 111.84 and 133.77).

### 2.3. The crystal structures of *4* and *6*

View of the molecular structure of **4** is shown in Fig. 1 and the selected geometric data are listed in Table 1. The coordination environment around the Fe(2) atom is regular trigonal pyramidal as evidenced by the interligand angles (Table 1) and also by the τ parameter of 0.93 (the value expected for ideal trigonal bipyramid is 1.0) [21]. The Fe(2)-donor distances compare favourably to the respective distances reported for [Fe(CO)$_4$(dppf-κ*P*)] (Fe–P 2.243(3) Å, Fe–CO 1.75(1)–1.79(1) Å [13]), [(μ-dppf)-{Fe(CO)$_4$}$_2$] (Fe–P 2.251(5) Å, Fe–CO 1.78(2)–1.79(2) Å [13]), and [Fe(CO)$_4$(Ph$_2$PfcCONEt$_2$-κ*P*)] (Fe–P 2.2505(6) Å, Fe–CO 1.787(2)–1.800(2) Å [15]).

The Fe(CO)$_4$ fragment is located at the side of the ferrocene moiety so that the equatorial plane [FeC(*n*)O(*n*)] (*n* = 2–4) is nearly perpendicular to the Cp(1) ring (the dihedral angle is 85.3(2)°). Consequently, the Fe(2)–P vector deviates only by 3.4(2)° from the Cp(1) plane, with the phosphorus and Fe(2) atoms being displaced by 0.159(1) and 0.289(1) Å, respectively, above the Cp(1) plane (i.e., away from the ferrocene iron atom). To minimise steric interactions, the Fe(2)(CO)$_3$ and 'PC$_3$' moieties are mutually staggered with the O*C*–Fe(2)–P–*C*(Ph) dihedral angles close to 60°.

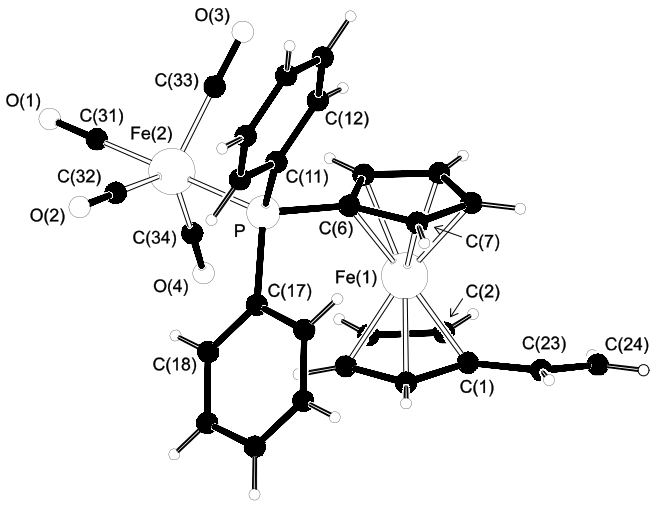


Fig. 1. Molecular structure of **4** showing the atom labeling scheme. Carbon atoms within the aromatic rings are numbered consecutively and, hence, only the pivotal and their adjacent carbon atoms are labelled for clarity.

Table 1
Selected interatomic distances and angles for **4** (in Å and °)[a]

| | |
|---|---|
| Fe(2)–P | 2.237(1) |
| Fe(2)–C(31) | 1.793(3) |
| Fe(2)–C(32) | 1.798(4) |
| Fe(2)–C(33) | 1.779(3) |
| Fe(2)–C(34) | 1.756(4) |
| O(1)–C(31) | 1.147(4) |
| O(2)–C(32) | 1.150(5) |
| O(3)–C(33) | 1.156(4) |
| O(4)–C(34) | 1.172(4) |
| P–C(6) | 1.803(3) |
| P–C(11) | 1.815(4) |
| P–C(17) | 1.828(4) |
| C(1)–C(23) | 1.451(6) |
| C(23)–C(24) | 1.321(6) |
| P–Fe(2)–C(31) | 178.6(1) |
| P–Fe(2)–C(eq)[b] | 87.1(1)–89.8(1) |
| Fe(2)–C–O[c] | 177.4(3)–179.6(3) |
| C(31)–Fe(2)–C(eq)[d] | 90.7(2)–92.6(2) |
| C(eq)–Fe(2)–C(eq)[e] | 118.2(2)–122.7(2) |
| C–P–C[f] | 102.9(2)–105.8(2) |
| C(1)–C(23)–C(24) | 125.1(4) |
| Fe(1)–Cg(1) | 1.655(2) |
| Fe(1)–Cg(2) | 1.650(2) |
| ∠Cp1,Cp2 | 4.1(2) |

[a] The ring planes are defines as follows: Cp(1), C(1–5); and Cp(2), C(6–10). Cg(1,2) denote the respective ring centroids.
[b] The range of P–Fe(2)–C(32,33,34) angles.
[c] The range of Fe(2)–C(*n*)–O(*n*) angles, where *n* = 31–34.
[d] The range of C(31)–Fe(2)–C(32,33,34).
[e] The range of C(32)–Fe(2)–C(33,34) and C(33)–Fe(2)–C(34) angles.
[f] The range of C(6)–P–C(11,17) and C(11)–P–C(17) angles.

The ferrocene unit shows practically identical Fe-ring centroid distances and a tilt of 4.1(2)° with the side proximal to the $Fe(CO)_4$ unit being more opened for steric reasons. The two ferrocene substituents are rotated with the torsion angle C(1)–Cg(1)–Cg(2)–C(6) of 136°, which corresponds to an intermediate conformation between anti-staggered and anti-eclipsed (cf. the ideal values of 108° and 144°, respectively). The vinyl group is slightly rotated from the plane of its bonding cyclopentadienyl ring: The angle subtended by the Cp(2) plane and the C(23)–C(24) bond is 11.8(3)°.

View of the molecular structure of **6** is presented in Fig. 2 and the selected geometric data are given in Table 2. Complex **6** crystallises with the symmetry of the monoclinic $P2_1/c$ space group with the tungsten atom residing on the crystallographic inversion centers, which renders only the half of the molecule symmetrically independent. The interligand angles around the tungsten atom differ only marginally from octahedral ones irrespective of the unlike W-donor bond lengths (cf. P–W–C(31,32) angles in Table 1). The observed W–P distance (2.4816(8) Å) is noticeably shorter than those reported for other structurally characterised complexes with ferrocene ligands featuring either terminal $W(CO)_5$ units (e.g., $[Cl_2Pt\{(\mu\text{-dppf})W(CO)_5\}_2]$, W–P 2.546(6) Å [22]; $[W(CO)_4(L\text{-}\kappa P)]$, where L = ($S_p$)-1-(diphenylphosphanyl)-2-((*E*)-2-phenyethenyl)ferrocene, W–P 2.562(1) and 2.547(1) Å [9]; and $[(OC)_5W{=}C(NEt_2)\text{-}fcPPh_2W(CO)_5]$ *W*–P 2.545(1) Å [15]) or chelated $W(CO)_4$ moieties ($[W(CO)_4(L\text{-}\eta^2{:}\kappa P)]$, where L = ($S_p$)-1-(diphenylphosphanyl)-2-vinylferrocene, W–P 2.5328(9) Å [9a]; $[W(CO)_4(dppf\text{-}\kappa^2 P,P')]$, W–P 2.533(2) and 2.563(2) Å [23]; and $[W(CO)_4(Ph_2PfcC(NEt_2)\text{-}\kappa^2 C^1,P)]$, W–P 2.5391(9) Å [15]). By contrast, the W–CO distances found in **6** do not differ much from those in the mentioned complexes.

Table 2
Selected interatomic distances and angles for **6** (in Å and °)[a]

| | |
|---|---|
| W–P | 2.4816(8) |
| W–C(31) | 2.025(4) |
| W–C(32) | 2.029(4) |
| O(1)–C(31) | 1.147(5) |
| O(2)–C(32) | 1.147(5) |
| P–C(6) | 1.816(4) |
| P–C(11) | 1.838(4) |
| P–C(17) | 1.848(4) |
| C(1)–C(23) | 1.43(1) |
| P–W–C(31) | 90.8(1) |
| P–W–C(32) | 84.4(1) |
| W–C(31)–O(1) | 178.8(3) |
| W–C(32)–O(2) | 177.4(4) |
| W–P–C[b] | 112.2(1)–121.7(1) |
| C–P–C[c] | 100.0(2)–101.1(2) |
| Fe–Cg(1) | 1.652(3) |
| Fe–Cg(2) | 1.646(2) |
| ∠Cp1,Cp2 | 3.2(3) |

[a] The ring planes are defines as follows: Cp(1), C(1–5); and Cp(2), C(6–10). Cg(1,2) denote the respective ring centroids.
[b] The range of W–P–C(6,11,17) angles.
[c] The range of C(6)–P–C(11,17) and C(11)–P–C(17) angles.

The ferrocene Cp(2) and the $\{WC_4\}$ planes in **6** are practically perpendicular (the dihedral angle is 88.9(2)°). Owing to the imposed symmetry and the overall molecular conformation, the ligand moieties are centrosymmetric images (i.e., are anti to each other) and their '$PC_3$' motifs appear mutually staggered (i.e., rotated by ca. 60°) when looked upon along the P–P′ line. Similarly to **4**, the ferrocene cyclopentadienyls exert a tilt of 3.2(2)° and adopt an intermediate conformation between anti-staggered and anti-eclipsed with the torsion angle C(1)–Cg(1)–Cg(2)–C(6) = 130°.

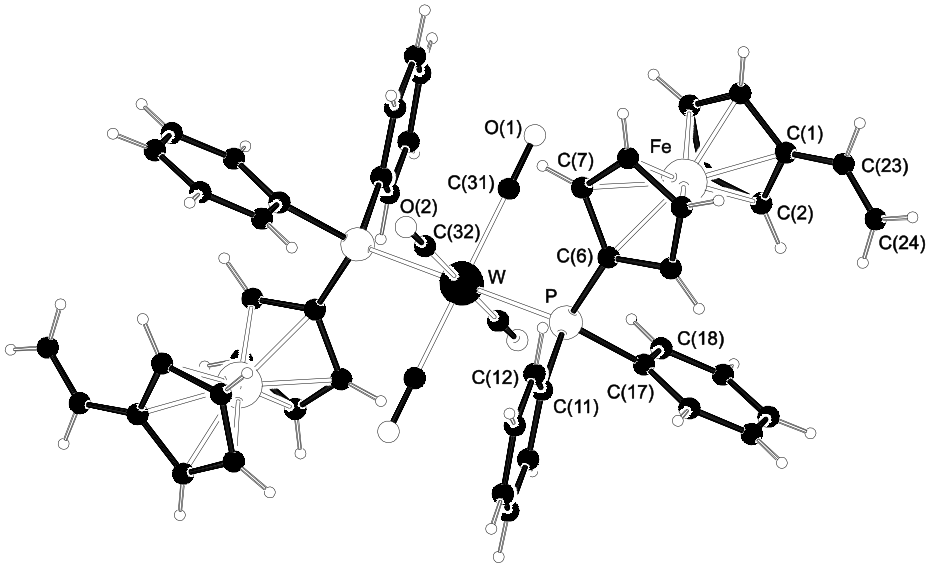


Fig. 2. View of the molecular structure of **6**. For clarity, only labels for the pivotal and their adjacent carbon atoms with the consecutively numbered aromatic rings are shown. The non-labeled part of the molecule is generated by the crystallographic inversion operation (symmetry operation: $1/2 - x$, $3/2 - y$, $-z$).

### 2.4. Electrochemistry

The electrochemical behaviour of **1**, **2**, **4** and **6** has been studied by cyclic voltammetry on platinum disc electrode in ca. 0.5 mM dichloromethane solutions containing 0.1 M $Bu_4NPF_6$ as the supporting electrolyte. The electrochemical data are summarised in Table 3.

Compound **1** becomes oxidised in a single irreversible step (Fig. 3), attributable to oxidation of the ferrocene moiety to the corresponding ferrocenium. Because of the presence of electron-withdrawing substituents, the oxidation of **1** appears at more positive potentials than that of ferrocene itself [$E_{pa} = 0.12$ V vs. ferrocene/ferrocenium at the scan rate 0.1 V $s^{-1}$; $E_{pa}$ ($E_{pc}$) are the anodic (cathodic) peak potentials]. The process is diffusion controlled as indicated by the peak current ∝ (scan rate)$^{1/2}$ over the range 0.1–5 V $s^{-1}$ but is associated with follow-up processes that convert the electro-generated product into another (redox active) species (see Fig. 4). Accordingly, a minor wave was observed at higher potentials, which becomes more pronounced during repeated cycling and is associated with a reductive counterwave ($E_{pa} = 0.27$ V, $E_{pc} = 0.20$ V vs. ferrocene/ferrocenium). The peak couple can be attributed to oxidation of the corresponding phosphane oxide present as a trace impurity in **1** or, more likely, formed by reaction of the electrochemically generated cation radical $\mathbf{1}^{+\cdot}$ with traces of oxygen or water [24].

The redox behaviour of **2** is very similar except that the oxidation shows signs of reversibility. At scan rates up to 5 V $s^{-1}$, the current ratio $i_{pa}/i_{pc}$ is always lower than unity but increases with the scan rate [$i_{pa}$ ($i_{pc}$) denotes the anodic (cathodic) peak current]. Compared to **1**, the oxidation of **2** is shifted by ca. 100 mV more positive ($E_{pa} = 0.22$ V vs. ferrocene/ferrocenium at scan rate 0.1 V $s^{-1}$; Fig. 3).

Table 3
Summary of the electrochemical data[a]

| Compound | $E^{\circ\prime}$ [V] |
|---|---|
| **1** | +0.12[b] |
| **2** | +0.21 |
| **4** | +0.28,[c] +0.58[b] |
| **6** | +0.17, +0.82,[b] ca. +1.27 |

[a] The potentials are given relative to ferrocene/ferrocenium reference. See Section 4 for details.
[b] Irreversible oxidation. Oxidation peak potential ($E_{pa}$) given (0.1 V $s^{-1}$).
[c] See text.

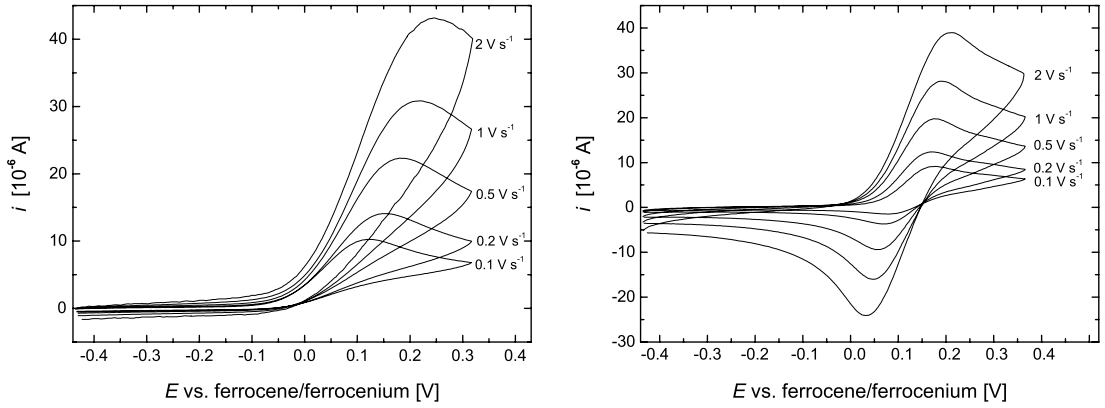


Fig. 3. Cyclic voltammograms of 0.5 mM dichloromethane solutions of **1** (left) and **2** (right) as recorded on platinum disc electrode at varying scan rate.

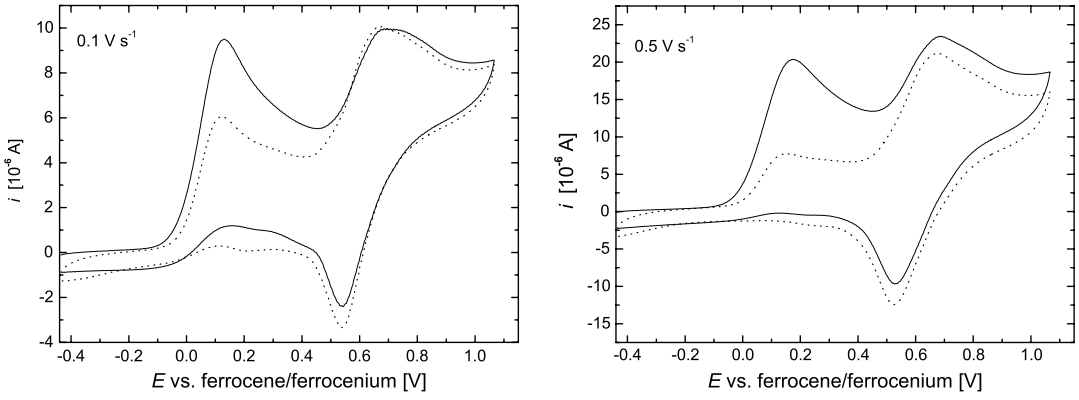


Fig. 4. Cyclic voltammograms of **1** recorded at different scan rates (left 0.1 V $s^{-1}$, right 0.5 V $s^{-1}$). The response obtained in the first cycle is shown in full line while the second scan is indicated with a dotted line. Conditions: Pt disc electrode, 0.5 mM dichloromethane solution.

The oxidation of the dinuclear complex **4** occurs in two separated one-electron steps. The first oxidation is reversible and occurs most likely at the ferrocene ligand. The shift towards more positive potentials can be accounted for by an electron density lowering at the ferrocene unit connected with coordination (Table 3). The following oxidation is irreversible as well and can be tentatively attributed to an oxidation of the $Fe(CO)_4$ fragment (Fig. 5). A similar two-step oxidative behaviour has been reported for $[Fe(CO)_4(L\text{-}\kappa P)]$, where $L = [Fe(\eta^5\text{:}\eta^5\text{-}C_5H_4CH_2CH_2P(Ph)CH_2CH_2C_5H_4)]$ [25].

During scanning over both oxidative processes at relatively slow scan rates (e.g., 0.1 V $s^{-1}$), a post-peak emerges after the second wave while the reductive wave corresponding to the first redox step occurs with a peak current lower than for the respective oxidation counter wave. When the scan rate is kept at 0.1 V $s^{-1}$ and the switching potential is increased, an additional oxidation wave appears at around +1.26 V during the second cycle while the original peaks nearly disappear from the cyclic voltammogram (Fig. 5). As the overall reversibility increases at higher scan rates, it is likely that the oxidation of **4** is accompanied by some chemical complications and, probably, adsorption at the electrode surface.

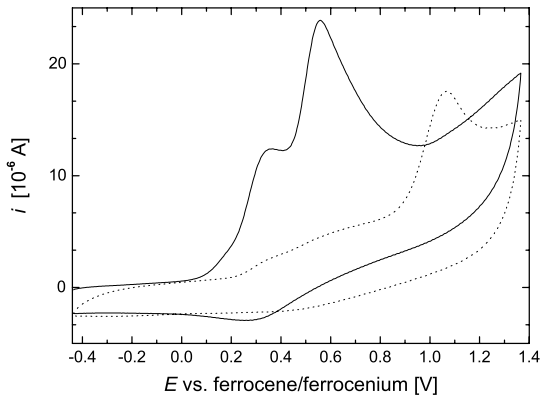


Fig. 5. Cyclic voltammograms of **4** as recorded on a platinum disc electrode for 0.5 mM dichloromethane solutions and at 0.1 V $s^{-1}$ scan rate. Note the difference between the first (solid line) and the second cycle (dotted line).

The redox response of compound **6** parallels the behaviour of $[W(CO)_4(FcPPh_2\text{-}\kappa P)_2]$ [26] in that it undergoes two successive, well-separated ferrocene oxidations followed by a third, tungsten-centered one. The first ferrocene oxidation is observed with full reversibility while the second and third are essentially irreversible (Fig. 6). Similarly to **4**, the redox steps are coupled with processes that result in blocking of the electrode surface (Fig. 6).

The potential of the tungsten-centered oxidation in **6** is markedly higher than that reported for $[W(CO)_4(PPh_3)_2]$ (ca. 0.45 V vs. ferrocene/ferrocenium; irreversible wave) [27]. This shift, apparently contrasting with the donor ability of the ligands (ferrocenyl is a strong electron-donating group), can be rationalised by the sequence of the redox steps. Whereas the phosphane donors in $[W(CO)_4(PPh_3)_2]$ are redox-silent, compound **6** undergoes firstly two ferrocene-based oxidations that convert neutral **6** to a dicationic bis(ferrocenium) species. Thus, the species to be oxidised in the last step is not only positively charged but also contains two ligands whose donor ability has been changed during the preceding redox steps (electron-donating ferrocene becomes electron-withdrawing ferricinium; cf. the Hammett $\sigma_p$ constants −0.18 and 0.29 for the ferrocenyl and ferrocenium groups, respectively) [28], which naturally influences the redox response of the 'central' atom.

## 3. Conclusions

Organometallic phosphanylalkenes **1** and **2** readily coordinate to '$M(CO)_4$' fragments (M = W and Fe) as P-monodentate donors, while the alkenyl groups act as spectator peripheral substituents. The reluctance of **1** and **2** to form chelate complexes, already demonstrated in a series of palladium(II) and copper(I) complexes [8], stands against the

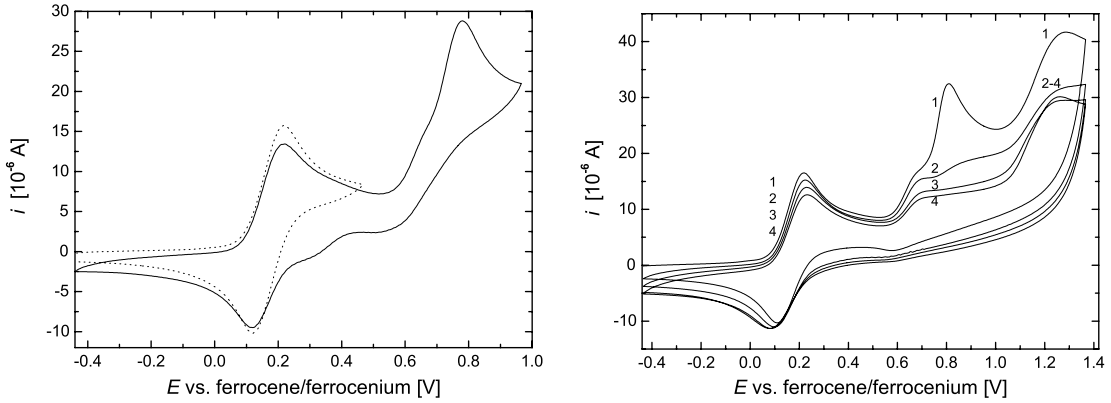


Fig. 6. (left) Cyclic voltammograms of **6** as recorded on a platinum disc electrode for 0.5 mM dichloromethane solution at 0.1 V $s^{-1}$ scan rate. The dotted line indicates the scan limited to the first oxidation. (right) Changes in cyclic voltammograms of **6** upon repeated cycling at 0.1 V $s^{-1}$ scan rate (the first four scans, 1–4 are shown).

coordination behaviour of their 1,2-analogues [9a] and organyls containing the 1′-(diphenylphosphanyl)ferrocen-1-yl group: 1′-(diphenylphosphanyl)ferrocen-1-yl [29] and [1′-(diphenylphosphanyl)ferrocenyl]methylidene [15,30]. The structures of the resulting metal-carbonyl complexes were established by spectral methods and, for crystalline compounds, confirmed by X-ray diffraction analysis. In addition, the redox behaviour of the selected representatives has been studied by cyclic voltammetry on platinum disc electrode.

## 4. Experimental

### 4.1. Materials and methods

All syntheses were performed under argon atmosphere. Tetrahydrofurane (THF) was distilled from potassium/benzophenone ketyl. Toluene was dried over sodium metal and distilled. Compounds **1** [18] and 1,1′-dibromoferrocene [11b] were prepared by the literature procedures. Other chemicals and solvents for chromatography were obtained from commercial sources and used without purification (Fluka, Aldrich; solvents from Lach-Ner). The reported yields are not optimised.

NMR spectra were recorded on a Varian UNITY Inova 400 spectrometer ($^{1}$H, 399.95; $^{13}$C, 100.58; $^{31}$P, 161.90 MHz) at 298 K. Chemical shifts ($\delta$/ppm) are given relative to internal tetramethylsilane ($^{1}$H and $^{13}$C) or an external 85% aqueous $H_3PO_4$ ($^{31}$P). The second-order multiplets due to the alkenyl- (AA′BB′ spin system) and phosphanyl-substituted (AA′BB′X spin system) ferrocene cyclopentadienyl rings are labelled as apparent triplets and quarterts (Fc = ferrocenyl, fc = ferrocene-1,1′-diyl). IR spectra were measured on an FT IR Nicolet Magna 760 instrument in the range of 400–4000 cm$^{-1}$. Mass spectra in EI and FAB mode were recorded with a ZAB-EQ (VG Analytical) spectrometer. The complexes notoriously give erratic results in the standard combustion analysis due to their limited stability and/or incomplete combustion.

Electrochemical measurements were carried out with a computer-controlled multipurpose polarograph μAUTOLAB III (Eco Chemie) at room temperature using a standard three-electrode cell with rotating platinum disc electrode (AUTOLAB RDE; 3 mm diameter) as the working electrode, platinum sheet auxiliary electrode, and calomel reference electrode (3 M KCl). The analysed compounds were dissolved in dichloromethane (Fluka, absolute, declared $H_2O$ content below 0.005%) to give $5 \times 10^{-4}$ M concentration of the analyte and 0.1 M $Bu_4NPF_6$ (Fluka, purissimum for electrochemistry). The solutions were deaerated with argon prior to the measurement and then kept under an argon blanket. The redox potentials are given relative to the ferrocene/ferrocenium reference and are reproducible within ca. ±5 mV. The potential of the ferrocene/ferrocenium couple under the experiment conditions was +0.435 V.

### 4.2. Preparation of 1′-dimethylvinylsilyl-1-bromoferrocene (3)

Butyl lithium (2.0 mL of 2.5 M solution in hexanes, 5.0 mmol) was added to a solution of 1,1′-dibromoferrocene (1.72 g, 5.0 mmol) in dry THF (20 mL) with cooling to −78 °C (dry ice/ethanol bath). The mixture was stirred at this temperature for 10 min whereupon an orange precipitate formed. Chlorodimethyl(vinyl)silane (0.8 mL, 6 mmol) was slowly added causing the precipitate to dissolve, and the formed dark yellow-brown solution was stirred at −78 °C for 15 min and then at room temperature for 90 min. Then, the reaction mixture was quenched by addition of saturated aqueous $NaHCO_3$ solution. The organic layer was separated, washed with brine, dried ($MgSO_4$) and evaporated, leaving the crude product as a dark amber oil. Subsequent purification by flash column chromatography (silica gel, hexane) afforded silane **3** as an amber orange oil. Yield: 1.532 g (88%). The product is typically contaminated by trace amounts of side products such as $FcSiMe_2(CH{=}CH_2)$, FcBr, and unreacted $fcBr_2$, which cannot be effectively removed by chromatography due to similar retention characteristics. However, the side products do not hamper the following step and their amounts are conveniently reduced by chromatography after the subsequent phosphanylation (see the following section).

$^{1}$H NMR ($CDCl_3$): $\delta$ 0.32 (s, 6H, $SiMe_2$), 4.05, 4.10, 4.37, 4.40 (4 × apparent t, 2H, fc); 5.73 (dd, $^{2}J_{HH} = 3.7$, $^{3}J_{HH} = 20.3$ Hz, 1H, $=CH_2$), 6.00 (dd, $^{2}J_{HH} = 3.7$, $^{3}J_{HH} = 14.6$ Hz, 1H, $=CH_2$), 6.30 (dd, $^{3}J_{HH} = 14.6$, 20.3 Hz, 1H, =CH). $^{13}$C{$^{1}$H} NMR ($CDCl_3$): $\delta$ −2.03 ($SiMe_2$), 67.33, 70.31 (2 × CH of fc); 71.62 (C–Si of fc), 74.09, 75.65 (2 × CH of fc); 77.70 (C–Br of fc), 131.87 ($=CH_2$), 138.69 (=CH). EI MS: *m*/*z* (relative abundance) 350 (97), 348 (100) ($M^{+\cdot}$); 270 (12, $[M-Br]^+$), 186 (11), 184 (10), 121 (16, $C_5H_5Fe^+$), 85 (31, $(CH_2CH)Me_2Si^+$). HR MS: for $C_{14}H_{17}\,^{79}Br^{56}FeSi$ ($M^+$) calc. 347.9632; found, 347.9642.

### 4.3. Preparation of 1′-dimethylvinylsilyl-1-(diphenylphosphanyl)ferrocene (2)

Butyl lithium (1.7 mL of 2.5 M solution in hexanes, 4.3 mmol) was added to a solution of **3** (1.36 g, 3.9 mmol) in dry THF (10 mL) while cooling to −78 °C (dry ice/ethanol bath). After stirring for 15 min, neat chlorodiphenylphosphane (0.9 mL, 4.9 mmol) was added dropwise and the resulting mixture was stirred at −78 °C for 15 min and then at room temperature for 90 min. The reaction was terminated by addition of saturated aqueous $NaHCO_3$ solution and stirring for another 30 min. The reaction mixture was diluted with diethyl ether, the organic layer was separated, washed with brine, dried ($MgSO_4$), and concentrated under vacuum. The brown residue was purified by column chromatography on silica gel. First, elution with hexane removed a minor orange band due to side products. The following elution with hexane–diethyl ether (1:9 v/v)

afforded the major orange band of the product. Evaporation of the second band under vacuum yielded **2** as an orange brown oil. Yield: 1.21 g (68%, calculated for pure **3**). Chromatographic purification markedly reduces the amount of impurities mentioned above; another side product formed during the phosphanylation step, detectable by NMR and GC–MS is (diphenylphosphanyl)ferrocene.

$^1$H NMR ($CDCl_3$): $\delta$ 0.25 (s, 6H, $SiMe_2$), 4.01 (apparent t, 2H), 4.07 (apparent q, 2H), 4.19 (apparent t, 2H), 4.33 (apparent t, 2H) (4 × CH of fc); 5.68 (dd, $^2J_{HH} = 3.7$, $^3J_{HH} = 20.3$ Hz, 1H, =$CH_2$), 5.96 (dd, $^2J_{HH} = 3.7$, $^3J_{HH} = 14.6$ Hz, 1H, =$CH_2$), 6.23 (dd, $^3J_{HH} = 14.6$, 20.3 Hz, 1H, =CH), 7.27–7.40 (m, 10H, $PPh_2$). $^{13}C\{^1H\}$ NMR ($CDCl_3$): $\delta$ −2.08 ($SiMe_2$), 70.62 (C–Si of fc), 71.13 (d, $J_{PC} = 4$ Hz), 72.37 (d, $J_{PC} \approx 1$ Hz), 72.98 (d, $J_{PC} = 15$ Hz), 74.03 (4 × CH of fc); 75.83 (d, $^1J_{PC} = 7$ Hz, C–P of fc), 128.08 (d, $J_{PC} = 7$ Hz, CH of $PPh_2$), 128.43 (CH of $PPh_2$), 131.68 (=$CH_2$), 133.46 (d, $J_{PC} = 20$ Hz, CH of $PPh_2$), 138.85 (=CH), 139.09 (d, $^1J_{PC} = 10$ Hz, $C_{ipso}$ of $PPh_2$). $^{31}P\{^1H\}$ NMR ($CDCl_3$): $\delta$ −16.3 (s). EI MS: *m*/*z* (relative abundance) 454 (100, $M^+$), 370 (35, $[FcPPh_2]^{+\cdot}$), 242 (18), 240 (13), 199 (15), 183 (17). HR MS: for $C_{26}H_{27}{}^{56}FePSi$ ($M^+$) calc. 454.0969; found, 454.0980.

### 4.4. Preparation of tetracarbonyl-[1-(diphenylphosphanyl-κP)-1′-vinylferrocene]iron(0) (4)

A mixture of $[Fe_2(CO)_9]$ (73 mg, 0.20 mmol), **1** (80 mg, 0.20 mmol) and toluene (1 mL) was brought to boiling whereupon the solid carbonyl quickly dissolved to give a turbid orange solution. After refluxing for 1 h, the reaction mixture was cooled to room temperature and passed trough a short silica gel column (elution with toluene) to remove dark decomposition products. The orange eluate was evaporated under vacuum and the residue immediately dissolved in hot heptane (4 mL). The solution was filtered while hot and the filtrate was allowed to crystallise at room temperature and then 0 °C overnight. The formed crystals were isolated by suction, washed with cold pentane and dried under vacuum to give **4** as an orange crystalline solid (fine needles). Yield: 94 mg, 83%.

$^1$H NMR ($CDCl_3$): $\delta$ 3.73, 4.02 (2 × apparent t, 2H), 4.42 (m, 2H), 4.46 (apparent q, 2H) (4 × CH of fc); 4.95 (dd, $^3J_{HH} = 10.8$, $^2J_{HH} = 1.3$ Hz, 1H, =$CH_2$), 5.18 (dd, $^3J_{HH} = 17.5$, $^2J_{HH} = 1.3$ Hz, 1H, =$CH_2$), 6.02 (dd, $^3J_{HH} = 17.5$, 10.8 Hz, 1H, =CH), 7.38–7.59 (m, 10H, $PPh_2$). $^{13}C\{^1H\}$ NMR ($CDCl_3$): $\delta$ 67.91, 71.32, 74.05 (d, $J_{PC} = 9$ Hz), 75.38 (d, $J_{PC} = 12$ Hz) (4 × CH of fc); 84.68 (*C*CH=$CH_2$ of fc), 112.41 (=$CH_2$), 128.13 (d, $J_{PC} =$ 10 Hz), 130.36 (d, $J_{PC} = 2$ Hz), 132.52 (d, $J_{PC} = 10$ Hz) (3 × CH of $PPh_2$); 133.33 (=CH), 137.72 (d, $^1J_{PC} = 52$ Hz, $C_{ipso}$ of $PPh_2$), 213.30 (d, $^2J_{PC} = 19$ Hz, C≡O); the *C*P signal of fc was not found, probably due to overlaps with the solvent signal. $^{31}P\{^1H\}$ NMR ($CDCl_3$): $\delta$ +66.7 (s). IR (Nujol): $\nu$/cm$^{-1}$ $\nu$(C≡O) 2049 (vs), 1979 (vs), 1944 (br vs), 1906 (br vs). EI MS: *m*/*z* (relative abundance) 564 (10, $M^{+\cdot}$), 508 (9, $[M-2CO]^{+\cdot}$), 478 (8), 452 (96, $[M-4CO]^{+\cdot}$), 426 (20, $[M-4CO-C_2H_2]^{+\cdot}$), 396 (100, $\mathbf{1}^{+\cdot}$), 370 (51, $[\mathbf{1}–C_2H_2]^{+\cdot}$, isobaric with $FcPPh_2{}^{+\cdot}$). HR MS: calc. for $C_{28}H_{21}{}^{56}Fe_2O_4P$ ($M^{+\cdot}$), 563.9876; found, 563.9901.

### 4.5. Preparation of tetracarbonyl-[1-(diphenylphosphanyl-κP)-1′-(dimethylvinylsilyl)ferrocene]iron(0) (5)

A mixture of $[Fe_2(CO)_9]$ (72 mg, 0.20 mmol), **2** (92 mg, 0.20 mmol) and toluene (8 mL) was heated at reflux for 1 h. The mixture was cooled, evaporated under vacuum and the residue was purified by column chromatography (silica gel, hexane–diethyl ether 5:1). Collecting the major band followed by evaporation gave pure **6** as an orange glassy solid. Yield: 88 mg (71%).

$^1$H NMR ($CDCl_3$): $\delta$ 0.21 (s, 6H, $SiMe_2$), 3.74 and 3.77 (2 × apparent t, 2H, fc); 4.48–4.51 (m, 4H, fc), 5.66 (dd, $^3J_{HH} = 20.2$, $^2J_{HH} = 3.8$ Hz, 1H, =$CH_2$), 5.97 (dd, $^3J_{HH} =$ 14.6, $^2J_{HH} = 3.8$ Hz, 1H, =$CH_2$), 6.18 (dd, $^3J_{HH} = 20.2$, 14.6 Hz, 1H, =CH), 7.39–7.57 (m, 10H, $PPh_2$). $^{13}C\{^1H\}$ NMR ($CDCl_3$): $\delta$ −2.18 ($SiMe_2$), 71.39 (*C*Si of fc), 72.08 (d, $J_{PC} = 9$ Hz), 73.86, 74.11, 74.73 (d, $J_{PC} = 12$ Hz) (4 × CH of fc); 128.10 (d, $J_{PC} = 10$ Hz), 130.37 (d, $J_{PC} = 2$ Hz) (2 × CH of $PPh_2$); 132.05 (=$CH_2$), 132.53 (d, $J_{PC} = 10$ Hz, CH of $PPh_2$), 137.43 (=CH), 138.12 (d, $^1J_{PC} = 33$ Hz, $C_{ipso}$ of $PPh_2$), 213.27 (d, $^2J_{PC} = 20$ Hz, C≡O); the signal due to *C*P of fc is probably obscured by the solvent resonance. $^{31}P\{^1H\}$ NMR ($CDCl_3$): $\delta$ +67.0 (s). IR (RAS): $\nu$/cm$^{-1}$ $\nu$(C≡O) 2050 (vs), 2012 (w), 1975 (vs), 1952 (vs), 1913 (m). EI MS: *m*/*z* (relative abundance) 622 (4, $M^{+\cdot}$), 510 (58, $[M-4CO]^{+\cdot}$), 454 (100, $\mathbf{2}^{+\cdot}$), 370 (13, $[\mathbf{1}–SiMe_2(C_2H_2)]^{+\cdot}$, isobaric with $FcPPh_2{}^{+\cdot}$). HR MS: calc. for $C_{30}H_{27}{}^{56}Fe_2O_4PSi$ ($M^{+\cdot}$), 622.0115; found, 622.0105.

### 4.6. Preparation of trans-tetracarbonylbis[1-(diphenylphosphanyl-κP)-1′-vinylferrocene]tungsten(0) (6)

$[W(cod)(CO)_4]$ (41 mg, 0.10 mmol) and **1** (80 mg, 0.20 mmol) were dissolved in toluene (8 mL) and the solution was heated at gentle reflux for 3 h. Then, it was cooled to room temperature and filtered through a short silica gel column. The column was washed with toluene and the orange eluate was concentrated under vacuum. The glassy residue was immediately dissolved in hot heptane, the solution was filtered while hot and allowed to crystallise at room temperature and then at 0 °C. The separated crystalline product was filtered off, washed with hexane and dried under vacuum to give **6** as an orange microcrystalline solid. Yield: 82 mg (75%).

$^1$H NMR ($CDCl_3$): $\delta$ 3.94, 4.08 (2 × apparent t, 2H), 4.29 (br m, 2H), 4.35 (apparent t, 2H) (4 × CH of fc); 4.93 (dd, $^3J_{HH} = 10.7$, $^2J_{HH} = 1.6$ Hz, 1H, =$CH_2$), 5.18 (dd, $^3J_{HH} = 17.5$, $^2J_{HH} = 1.5$ Hz, 1H, =$CH_2$), 6.12 (dd, $^3J_{HH} = 17.5$, 10.7 Hz, 1 H, =CH), 7.31–7.56 (m, 10H, $PPh_2$). $^{13}C\{^1H\}$ NMR ($CDCl_3$): $\delta$ 67.73, 70.99, 73.23 (virtual t, $J' = 7$ Hz), 74.89 (virtual t, $J' = 6$ Hz) (4 × CH of fc); 82.49 (virtual t (1:1:1), $J' = 22$ Hz, *C*P of fc), 84.23

(*C*CH=$CH_2$ of fc), 111.84 (=$CH_2$), 127.53 (virtual t, $J' = 5$ Hz), 128.94, 132.61 (virtual t, $J' = 6$ Hz) (3 × CH of $PPh_2$); 133.77 (=CH), 140.48 (virtual t (1:1:1), $J' = 22$ Hz, $C_{ipso}$ of $PPh_2$), 204.05 (t, $^2J_{PC} = 6$ Hz, C≡O). $^{31}P\{^1H\}$ NMR ($CDCl_3$): $\delta$ +16.3 (s with $^{183}W$ satellites, $^1J_{WP} = 282$ Hz). IR (Nujol): $\nu/cm^{-1}$ $\nu$(C≡O) 1886 (vs), 1878 (vs), 1861 (sh). FAB MS: *m*/*z* 1088 ($M^+$). The compound shows very poorly abundant ions due to $M^+$ in its mass spectrum, not allowing for HR MS analysis.

### 4.7. Preparation of trans-tetracarbonylbis[1-(diphenylphosphanyl-κP)-1′-(dimethylvinylsilyl)ferrocene]tungsten(0) (7)

[W(cod)$(CO)_4$] (41 mg, 0.10 mmol) and **2** (92 mg, 0.20 mmol) were dissolved in toluene (8 mL) and the solution was heated at reflux for 3 h. The reaction mixture was cooled to room temperature, evaporated and the residue purified by column chromatography on silica gel using hexane–diethyl ether (5:1) as the eluent. The first and only orange band was collected and evaporated under vacuum to give **7** as an orange brown glassy solid. Yield: 98 mg (96%). The product is typically contaminated with [W$(CO)_5$(**2**)] (**8**) (5–15%).

$^1H$ NMR ($CDCl_3$): $\delta$ 0.18 (s, 6 H, $SiMe_2$), 3.74 and 4.11 (2 × apparent t, 2H, fc); 4.31 (m, 2H, fc), 4.42 (apparent t, 2H, fc), 5.63 (dd, $^3J_{HH} = 20.3$, $^2J_{HH} = 3.8$ Hz, 1H, =$CH_2$), 5.93 (dd, $^3J_{HH} = 14.6$, $^2J_{HH} = 3.8$ Hz, 1H, =$CH_2$), 6.16 (dd, $^3J_{HH} = 20.3$, 14.6 Hz, 1H, =CH), 7.12–7.57 (m, 10H, $PPh_2$). $^{13}C\{^1H\}$ NMR ($CDCl_3$): $\delta$ −2.15 ($SiMe_2$), 70.84 (*C*Si of fc), 71.31 (virtual t, $J' = 4$ Hz), 73.50, 73.89 (2 × CH of fc); 74.19 (virtual t, $J' = 5$ Hz, CH of fc), 82.22 (dd, $J_{PC} = 23$ and 21 Hz, *C*P of fc), 127.52 (virtual t, $J' = 5$ Hz), 128.95 (2 × CH of $PPh_2$); 131.70 (=$CH_2$), 132.61 (virtual t, $J' = 6$ Hz, CH of $PPh_2$), 138.64 (=CH), 140.5 (virtual t, $J' = 21$ Hz, $C_{ipso}$ of $PPh_2$), 204.08 (t, $^2J_{PC} = 6$ Hz, C≡O). $^{31}P\{^1H\}$ NMR ($CDCl_3$): $\delta$ +16.5 (s with $^{183}W$ satellites, $^1J_{WP} = 282$ Hz). HR MS calc. for $C_{56}H_{54}{}^{56}Fe_2O_4P_2Si_2{}^{184}W$, 1204.1244; found, 1204.1259.

NMR data for pentacarbonyl[1-(diphenylphosphanyl-κ*P*)-1′-(dimethylvinylsilyl)ferrocene]tungsten(0) (**8**). $^1H$ NMR ($CDCl_3$): $\delta$ 0.17 (s, 6H, $SiMe_2$), 3.82 and 4.16 (2 × apparent t, 2H, fc); 4.24 (apparent q, 2H, fc), 4.48 (f of apparent t, 2H, fc), 5.64 (dd, $^3J_{HH} = 20.1$, $^2J_{HH} = 3.8$ Hz, 1H, =$CH_2$), 5.95 (dd, $^3J_{HH} = 14.5$, $^2J_{HH} = 3.8$ Hz, 1H, =$CH_2$), 6.14 (dd, $^3J_{HH} = 20.1$, 14.5 Hz, 1H, =CH), 7.12–7.57 (m, 10H, $PPh_2$). $^{13}C\{^1H\}$ NMR ($CDCl_3$): $\delta$ 197.33 (d, $^2J_{PC} = 7$ Hz, four *cis*-C≡O), 207.77 (d, $^2J_{PC} = 20$ Hz, four *trans*-C≡O). $^{31}P\{^1H\}$ NMR ($CDCl_3$): $\delta$ +11.6 (s with $^{183}W$ satellites, $^1J_{WP} = 236$ Hz).

### 4.8. X-ray crystallography

Single crystals suitable for X-ray diffraction analysis were obtained by crystallisation from hot heptane (**4**: orange needle, $0.07 \times 0.09 \times 0.60$ mm$^3$) or from a toluene–heptane mixture (**6**: orange plate, $0.03 \times 0.10 \times 0.15$ mm$^3$).

Table 4
Crystallographic data, data collection and structure refinement parameters for **4** and **6**

| Compound | **4** | **6** |
|---|---|---|
| Formula | $C_{28}H_{21}Fe_2O_4P$ | $C_{52}H_{42}Fe_2O_4P_2W$ |
| $M$ (g mol$^{-1}$) | 564.12 | 1088.35 |
| Crystal system | Monoclinic | Monoclinic |
| Space group | $P2_1/c$ (no. 14) | $C2/c$ (no. 15) |
| $T$ (K) | 150(2) | 150(2) |
| $a$ (Å) | 13.3091(8) | 25.3510(5) |
| $b$ (Å) | 11.6271(7) | 9.4562(2) |
| $c$ (Å) | 15.6662(9) | 17.8789(4) |
| $\beta$ (°) | 92.208(5) | 95.499(1) |
| $V$ (Å$^3$) | 2422.5(2) | 4266.3(2) |
| $Z$ | 4 | 4 |
| $D_{calc}$ (g mL$^{-1}$) | 1.547 | 1.694 |
| $\mu$(Mo Kα) (mm$^{-1}$) | 1.297 | 3.484 |
| $T$[a] | 0.631–0.907 | 0.668–0.842 |
| Diffractions total | 27557 | 30981 |
| Unique/observed[c] diffractions | 5071/2199 | 4888/3610 |
| $R$ (observed data)[b,c] (%) | 4.09 | 3.03 |
| $R$, w$R$ (all data) (%)[c] | 12.97, 5.86 | 5.29, 6.76 |
| $\Delta\rho$ (e Å$^{-3}$) | 0.71, −0.47 | 0.57, −0.80 |
| CCDC entry | 660757 | 660758 |

[a] The range of transmission coefficients.
[b] Diffractions with $I_o > 2\sigma(I_o)$.
[c] $R = \Sigma||F_o| - |F_c||/\Sigma|F_o|$, $wR = [\Sigma w(F_o^2 - F_c^2)^2\}/\Sigma w(F_o^2)^2]^{1/2}$.

Full-set diffraction data for **4** ($\pm h \pm k \pm l$, $2\theta \leqslant 53°$) were collected with an Oxford Diffraction XCalibur 2 diffractometer with CCD detector Sapphire 2 equipped with an Oxford Instruments Cryojet HT Cooler and the data for **6** ($\pm h \pm k \pm l$, $2\theta \leqslant 55°$) were collected on a Nonius KappaCCD diffractometer equipped with a Cryostream Cooler (Oxford Cryosystems). The measurements were performed at 150(2) K with graphite monochromatised Mo Kα radiation ($\lambda = 0.71073$ Å). In both cases, the data were corrected for absorption using routines included in the diffractometer software. The ranges of transmission factors and all other relevant crystallographic data are given in Table 4.

The structures were solved by direct methods (SIR97 [31]) and refined by weighted full-matrix least squares on $F^2$ (SHELXL97 [32]). All non-hydrogen atoms were refined with anisotropic displacement parameters while the hydrogens were included in the calculated positions and refined using the "riding" model. Final geometric calculations were carried out with a recent version of PLATON program [33]. The calculated numerical values are rounded with respect to their estimated standard uncertainties given with one decimal.

## Acknowledgements

This study was financially supported by the Czech Science Foundation (Grant No. GA CR 203/05/0276) and is a part of the long-term research project supported by the Ministry of Education, Youth and Sports of the Czech Republic (Project No. MSM0021620857). The author is indebted to Dr. Ivana Císařová for recording the X-ray diffraction data.

## Appendix A. Supplementary material

CCDC 660757 and 660758 contain the supplementary crystallographic data for **4** and **6**. These data can be obtained free of charge from The Cambridge Crystallographic Data Centre via www.ccdc.cam.ac.uk/data_request/cif. Supplementary data associated with this article can be found, in the online version, at doi:10.1016/j.jorganchem.2007.10.056.

## References


[1] (a) L.H. Pignolet (Ed.), Homogeneous Catalysis with Metal Phosphine Complexes, Plenum Press, New York, 1983;
(b) C. Masters, Homogeneous Transition-metal Catalysis, A Gentle Art, University Press, Cambridge, 1981;
(c) J.H. Downing, M.B. Smith, in: J.A. McCleverty, T.J. Meyer (Eds.), Phosphorus Ligands in Comprehensive Coordination Chemistry, vol. 1, p. 254 (Chapter 1.12), Elsevier, Oxford 2003. Examples of phosphine complexes can be found in the whole compendium in the chapters dealing with the coordination chemistry of particular metals.

[2] For introductory information about phosphines modified with polar functional groups, see: (a) A. Bader, E. Lindner, Coord. Chem. Rev. 108 (1991) 27;
(b) C.S. Slone, D.A. Weinberger, C.A. Mirkin, Prog. Inorg. Chem. 48 (1999) 233.

[3] Selected examples: (a) M.A. Bennett, R.S. Nyholm, J.D. Saxby, J. Organomet. Chem. 10 (1967) 301;
(b) L.V. Interrante, G.V. Nelson, Inorg. Chem. 7 (1968) 2059;
(c) M.A. Bennett, W.R. Kneen, R.S. Nyholm, J. Organomet. Chem. 26 (1971) 293;
(d) P.R. Brookes, J. Organomet. Chem. 42 (1972) 459;
(e) G.B. Robertson, P.O. Whimp, J. Chem. Soc., Dalton Trans. (1973) 2454;
(f) M.A. Bennett, R.N. Johnson, I.B. Tomkins, J. Am. Chem. Soc. 96 (1974) 61;
(g) M.A. Bennett, R.N. Johnson, I.B. Tomkins, Inorg. Chem. 13 (1974) 346;
(h) M.A. Bennett, H.-K. Chee, J.C. Jeffery, G.B. Robertson, Inorg. Chem. 18 (1979) 1071;
(i) M.I. Bruce, T.W. Hambley, M.R. Snow, A.G. Swincer, J. Organomet. Chem. 273 (1984) 361, and references cited therein;
(j) M.A. Bennett, C. Chiraratvatana, G.B. Robertson, Organometallics 7 (1988) 1394;
(k) M.A. Bennett, C. Chiraratvatana, G.B. Robertson, U. Tooptakong, Organometallics 7 (1988) 1403;
(l) R.V. Parish, P. Boyer, A. Fowler, T.A. Kahn, W.I. Cross, R.G. Pritchard, J. Chem. Soc., Dalton Trans. (2000) 2287.

[4] Representative examples: (a) L.V. Interrante, M.A. Bennett, R.S. Nyholm, Inorg. Chem. 5 (1966) 2212;
(b) M.A. Bennett, W.R. Kneen, R.S. Nyholm, Inorg. Chem. 7 (1968) 556;
(c) M.A. Bennett, W.R. Kneen, R.S. Nyholm, Inorg. Chem. 7 (1968) 552, See also Refs. [3b,3c].

[5] (a) R. Shintani, W.-L. Duan, K. Okamoto, T. Hayashi, Tetrahedron Lett. 16 (2005) 3400;
(b) R. Shintani, W.-L. Duan, T. Nagano, A. Okada, T. Hayashi, Angew. Chem., Int. Ed. 44 (2005) 4611;
(c) W.-L. Duang, H. Iwamura, R. Shintani, T. Hayashi, J. Am. Chem. Soc. 129 (2007) 2130.

[6] (a) P. Marie, S. Deblon, F. Breher, J. Geier, C. Böhler, H. Rüegger, H. Schönberg, H. Grützmacher, Chem. Eur. J. 10 (2004) 4198;
(b) E. Piras, F. Läng, H. Rüegger, D. Stein, M. Wörle, H. Grützmacher, Chem. Eur. J. 12 (2006) 5849.

[7] Compound **1** has been reported previously as a by-product arising from acid-catalysed dehydration of 1-(diphenylphosphanyl)-1′-(1-hydroxyethyl)ferrocene and its reaction with $[(Cy_3P)_2Cl_2Ru{=}CHPh]$ (Cy = cyclohexyl) was studied: (a) I.R. Butler, W.R. Cullen, Can. J. Chem. 61 (1983) 147;
(b) I.R. Butler, S.J. Coles, M.B. Hursthouse, D.J. Roberts, N. Fujimoto, Inorg. Chem. Commun. 6 (2003) 760.

[8] P. Štěpnička, I. Císařová, Collect. Czech. Chem. Commun. 71 (2006) 215.

[9] (a) P. Štěpnička, I. Císařová, Inorg. Chem. 45 (2006) 8485;
(b) P. Štěpnička, M. Lamač, I. Císařová, J. Organomet. Chem., in press, doi:10.1016/j.jorganchem.2007.11.016.

[10] For a phosphane modified with the dimethylvinylsilyl group, see: E.C. Alyea, P.R. Meehan, G. Ferguson, S. Kannan, Polyhedron 16 (1997) 3479.

[11] (a) L.-L. Lai, T.-Y. Dong, Chem. Commun. (1994) 2347;
(b) T.-Y. Dong, L.-L. Lai, J. Organomet. Chem. 509 (1996) 131;
(c) I.R. Butler, R.L. Davies, Synthesis (1996) 1350.

[12] S.T. Chacon, W.R. Cullen, M.I. Bruce, O. bin Shawkataly, F.W.B. Einstein, R.H. Jones, A.C. Willis, Can. J. Chem. 68 (1990) 2001.

[13] T.-J. Kim, S.-C. Kwon, Y.-H. Kim, N.H. Heo, M.M. Teeter, A. Yamano, J. Organomet. Chem. 426 (1991) 71.

[14] T.S.A. Hor, L.-T. Phang, J. Organomet. Chem. 381 (1990) 121.

[15] L. Meca, D. Dvořák, J. Ludvík, I. Císařová, P. Štěpnička, Organometallics 23 (2004) 2541.

[16] U. Koelle, J. Organomet. Chem. 133 (1977) 53.

[17] L. Lukešová, J. Ludvík, I. Císařová, P. Štěpnička, Collect. Czech. Chem. Commun. 65 (2000) 1897.

[18] (a) P.S. Pregosin, R.W. Kunz, in: P. Diehl, E. Fluck, R. Kosfeld (Eds.), $^{31}P$ and C NMR Spectra of Transition Metal Phosphine Complexes in NMR Basic Principles and Progress, vol. 16, Sect. E, Springer, Berlin, 1979, p. 65, and references cited therein;
(b) W.H. Hersch, J. Chem. Educ. 74 (1997) 1485.

[19] P. Štěpnička, J. Podlaha, R. Gyepes, M. Polášek, J. Organomet. Chem. 552 (1998) 293.

[20] P. Štěpnička, I. Císařová, R. Gyepes, Eur. J. Inorg. Chem. (2006) 926.

[21] A.W. Addison, T.N. Rao, J. Reedijk, J. van Rijn, G.C. Verschoor, J. Chem. Soc., Dalton Trans. (1984) 1349.

[22] L.-T. Phang, S.C.F. Au-Yeung, T.S.A. Hor, S.B. Khoo, Z.-Y. Zhou, T.C.W. Mak, J. Chem. Soc., Dalton Trans. (1993) 165.

[23] L.-C. Song, J.-T. Liu, Q.-M. Hu, G.-F. Wang, P. Zanello, M. Fontani, Organometallics 19 (2000) 5342.

[24] J. Podlaha, P. Štěpnička, I. Císařová, J. Ludvík, Organometallics 15 (1996) 543.

[25] J.A. Adams, O.J. Curnow, G. Huttner, S.J. Smail, M.M. Turnbull, J. Organomet. Chem. 577 (1999) 44.

[26] J.C. Kotz, C.L. Nivert, J.M. Lieber, R.C. Reed, J. Organomet. Chem. 91 (1975) 87.

[27] J.W. Hershberger, R.J. Klinger, J.K. Kochi, J. Am. Chem. Soc. 104 (1982) 3034.

[28] C. Hansch, A. Leo, R.W. Taft, Chem. Rev. 91 (1991) 165.

[29] I.R. Butler, W.R. Cullen, Organometallics 3 (1984) 1846.

[30] (a) I.R. Butler, W.R. Cullen, F.W.B. Einsten, A.C. Willis, Organometallics 4 (1985) 603;
(b) I.R. Butler, S.J. Coles, M.B. Hursthouse, D.J. Roberts, N. Fujimoto, Inorg. Chem. Commun. 6 (2003) 760.

[31] A. Altomare, M.C. Burla, M. Camalli, G.L. Cascarano, C. Giacovazzo, A. Guagliardi, A.G.G. Moliterni, G. Polidori, R. Spagna, J. Appl. Crystallogr. 32 (1999) 115.

[32] G.M. Sheldrick, SHELXL97. Program for Crystal Structure Refinement from Diffraction Data, University of Gottingen, Germany, 1997.

[33] A.L. Spek, PLATON, a multipurpose crystallographic tool, Utrecht University, Utrecht, The Netherlands, 2007. Distributed via Internet at <http://www.cryst.chem.uu.nl/platon/>.